UNIVERSITY OF PITTSBURGH

ORTHOPAEDIC ROBOTICS LABORATORY

2023 SUMMER UNDERGRADUATE ABSTRACT BOOKLET

FOREWARD

The Orthopaedic Robotics Laboratory is the University of Pittsburgh's collaborative effort between the Department of Bioengineering and Department of Orthopaedic Surgery. The mission of the ORL is the prevention of degenerative joint diseases by improving diagnostic, repair, and rehabilitation procedures for musculoskeletal injuries using state-of-the-art robotic technology. The ORL would like to commend the work of the undergraduate students during the summer of 2023. Students made significant impacts in the study of shoulder and knee degenerative joint diseases. The work of our students, with the help of our mentors, contributes greatly to world of Orthopaedic Research and to all patients who benefit.

OUR TEAM

Jayson Baggett
Class of 2025
Bioengineering
University of Pittsburgh

Mark Morgan
Class of 2025
Bioengineering
University of Pittsburgh

Ryan Fry
Class of 2025
Bioengineering
University of Pittsburgh

TABLE OF CONTENTS

Determining Non-recoverable Strain in the Inferior Glenohumeral Ligament following Successive Anterior Dislocations

Mark Morgan[1]; Jumpei Inoue[2]; Tianyu Chen[2]; Ryan Fry[1]; Gillian Ahrendt[2]; Chan Hong Moon[3]; Volker Musahl[1,2]; Albert Lin[2]; Richard E. Debski[1,2]

1. Department of Bioengineering, University of Pittsburgh, Pittsburgh, PA
2. Department of Orthopaedic Surgery, University of Pittsburgh, Pittsburgh, PA
3. Department of Radiology, University of Pittsburgh, Pittsburgh, PA

INTRODUCTION: The glenohumeral joint is the most commonly dislocated joint in the human body with 80% of glenohumeral dislocations occurring anteriorly[1]. Bankart Repair with the addition of capsular plication is a common procedure for treatment of anterior dislocations[2]. However, recurrent instability of the glenohumeral joint following repair has been reported to be as high as 22%[3]. Currently, the procedure is subjective based on surgeon experience and qualitative observations which may explain the high recurrence rate[2]. Non-recoverable strain can be used as an indicator of capsular injury and can provide quantitative data about the optimal location and orientation for suture placement in a cadaveric model. In a previous study, a grid of markers was placed on the IGHL of cadaveric specimens and non-recoverable strain following multiple anterior dislocations of each specimen was determined from the change in the 3D coordinates of the markers between the intact and dislocated states[4]. The primary objective of this study was to determine and validate the magnitude of non-recoverable strain in the IGHL following multiple anterior dislocations on cadaveric models.

METHODS: 3 fresh frozen cadaveric specimens were dissected, removing all soft tissue and leaving the scapula, humerus, glenohumeral capsule, and the coracoacromial and coracohumeral ligaments. The scapula and humerus of each specimen were potted in clay in retroversion and a 7x11 grid of markers (gadolinium-soaked canola seeds) were placed on the inferior glenohumeral capsule to encompass the anterior band, axillary pouch, and posterior band. Shoulder specimens were mounted on a 6 degree of freedom robotic testing system and a universal force-moment sensor was used to measure forces in the specimens. Four cameras were connected to a DMAS 7 Motion Capture System (Spica Technology Corporation, Haiku, HI) to track the 3D coordinates of the 77 markers. The joint position that minimized the amounts of folds and wrinkles in the IGHL when the capsule was inflated with minimal pressure was used for the reference strain configuration. Five anterior dislocations were performed at 60 degrees of abduction and 60 degrees of external rotation as the majority of shoulder dislocations occur in abduction and external rotation[4]. The specimen was allowed to rest for 30 minutes following each dislocation. At the end of the five dislocations, the shoulder was returned to the determined reference strain configuration joint position to track marker coordinates. On ABAQUS (ABAQUS/CAE Student Edition 2022; Simulia, Providence RI), the non-recoverable strain across the IGHL in each specimen was calculated from the change in coordinates of the 77 markers in the reference and strained states. A model with 60 mesh elements was created for each specimen tested including the magnitude and direction of non-recoverable strain (**Figure 1**). The IGHL was divided into 8 sub-regions, the anterior band, the anterior axillary pouch, the posterior axillary pouch, and the posterior band, on both the glenoid and humeral sides. The average non-recoverable strain in each sub-region was calculated from the strain in the ABAQUS elements composing the region. A two sample t-test was used to compare the average strain between the previous and current study. Significance was set at $p<0.05$.

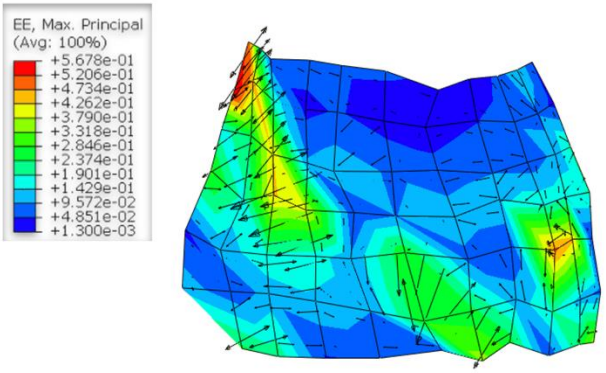

Figure 1. Representative contour model of non-recoverable strain. Orientation: glenoid side (top), humeral side (bottom), anterior (left), and posterior (right)

RESULTS: Across the 3 tests, the magnitude of non-recoverable strain ranged from 2.4% to 14.5% and peak non-recoverable strain by sub-region was between 10-15% (**Table 1**). During dislocation, any markers that fell or noticeably slipped were excluded which is noted in the table. A total of four markers were excluded across all tests. For test 1, the peak strain was 12.0% at the anterior band on the humeral side, test 2 had a peak strain of 14.5% at the anterior band on the glenoid side, and test 3 had a peak strain of 14.4% at the posterior band on the humeral side. To validate the non-recoverable strain results, a two sample t-test was performed comparing the peak strain values for the 3 tests to the peak strain values for the 8 tests of the previous study[4]. No difference in the peak strain values was found between datasets ($p>0.05$). The average minimum and maximum non-recoverable strain across all tests for each dataset was also compared and the differences between the averages was less than 3% (**Table 2**).

Table 1. Highest four regions of non-recoverable strain. Anterior band (AB), anterior axillary pouch (AAP), posterior axillary pouch (PAP), and posterior band (PB), on the glenoid (G) and humeral (H) sides. *One marker excluded from sub-region

Test	Sub-region	Strain (%)
1	ABH*	12.0
	PBG	11.7
	PAPG*	11.5
	AAPH	9.9
2	PBH*	14.9
	ABG*	14.5
	ABH	10.6
	AAPH	10.0
3	PBH	14.4
	PBG	11.9
	AAPG	8.5
	PAPG	7.4

Table 2. Average minimum and maximum non-recoverable strain for the current study and previous study[4].

	Average Min Strain (%)	Average Max Strain (%)
Current Study	3.9	13.8
Previous Study	1.4	11.1
Difference	2.5	2.7

DISCUSSION: Comparing results to those of previous study, the two sample, two-sided t-test showing no significant difference in peak strain values between the two datasets[4]. The repeatability of determining non-recoverable strain using the DMAS tracking system is within 3%[5]. Therefore, the differences between the average minimum and maximum strain values are not significant (**Table 2**). Both the location and magnitude of the highest four non-recoverable strain values varied greatly between specimens which underscores the importance of guiding clinical capsular plication with quantitative data. However, this methodology cannot be used for clinical patients post-dislocation. Surface area changes determined from MRI reconstructions on the IGHL may be a useful indicator of capsular injury. With the non-recoverable strain data from this study, a correlation between surface area changes and non-recoverable strain can be examined. Finding a correlation will lead the way to developing a clinical method of quantifying capsular injury through MRI.

SIGNIFICANCE: The determined non-recoverable strain data will be used to correlate surface area changes and strain on the cadaveric model. Clinical surface area data will then be used to develop a method of patient-specific capsular plication to improve patient outcomes following shoulder repair.

ACKNOWLEDGEMENTS: Support from the University of Pittsburgh Swanson School of Engineering, Department of Bioengineering, and Department of Orthopaedic Surgery is gratefully acknowledged.

REFERENCES:

[1] Hawkins et al. CORR, 1991
[2] Yoshida et al. JOR, 2022
[3] Bessiere et al. CORR, 2014
[4] Yoshida et al. JOR, 2020
[5] Moore et al., JOR, 2008

Characterizing the Morphology of the Inferior Glenohumeral Ligament following Multiple Anterior Dislocations

Ryan Fry[1,3], Jumpei Inoue MD[1], Tianyu Chen MS[1,2] Gillian Ahrendt MD [1,2], Zachary J. Herman MD [1,2]
Mark Morgan [1,3], Volker Musahl[1,2]; Albert Lin[2]; Richard E. Debski[1,2]
Chan-Hong Moon PhD[4], Volker Musahl MD[1,2], Albert Lin MD[1,2], Richard E. Debski PhD[1,2,3]
1. Orthopaedic Robotics Laboratory, University of Pittsburgh, Pittsburgh, PA
2. Department of Orthopedic Surgery, University of Pittsburgh, Pittsburgh, PA
3. Department of Bioengineering, University of Pittsburgh, Pittsburgh, PA
4. Department of Radiology, University of Pittsburgh, Pittsburgh, PA

INTRODUCTION: The glenohumeral joint is the most commonly dislocated joint in the human body, in which over 80% result from anterior dislocation[1]. Arthroscopic bankart repair is the most prevalent surgical repair procedure following anterior dislocation[2]. The inferior glenohumeral ligament (IGHL) prevents anterior dislocations, typically occurring in the glenohumeral joint's most vulnerable position, 90 degrees humeral-thoracic abduction and external rotation[3]. Following dislocation, the inferior glenohumeral capsule experiences non-recoverable strain, in addition to bankart lesions[4]. Due to injury reoccurring in 22% of cases and long-term instability, surgical intervention has become more prevalent to combat shoulder instability[2,5]. Modern capsulabral repair techniques include several types of anterior stabilization procedures, including capsular plication. Currently, capsular plication is performed based on the surgeon's experience, as there is not methodology to plicate specific subregions of the IGHL. Past literature has quantified capsular volume and found an increase in volume between patients that have experienced one or more anterior shoulder dislocations and those with healthy shoulders[6]. Surface area would also present an option for quantifying the capsular surface as this can be performed in vivo. Thus, the objective of this study is to characterize the surface area of the inferior glenohumeral ligament following multiple anterior dislocation using 3D geometric models generated from pre- and post-injury MRI data.

METHODS: Three fresh-frozen upper extremity cadavers (age 56.7 ± 1.9 years) were dissected, leaving only the humerus, scapula, and glenohumeral capsule. The specimens were potted, and a 7 x 11 grid of gadolinium-soaked canola seeds were glued onto the inferior glenohumeral ligament. The grid of markers divided the IGHL into eight subregions; anterior band, posterior band, anterior axillary pouch, and posterior axillary pouch, each having glenoid and humeral regions. Each shoulder was imaged via MRI using 3T (Siemens, mMR Biograph) and then mounted to the six degree of freedom robotic testing system in an optimal position showing minimal marker movement. The robot applied compressive and translational forces to simulate an anterior dislocation. The robot performed five dislocations allowing 30 minutes of rest between dislocations to minimize the effect of viscoelastic properties. Following dislocations, the specimens went through a post-dislocation MRI referenced as the dislocated state. Using Materialize MIMICS (version 25.0), each specimen was reconstructed into 3D geometric models consisting of the humerus, glenoid, glenohumeral capsule, and the 77 gadolinium-soaked canola seeds for the intact and dislocated state (**Figure 1**). Using MESHLAB (version 2020.07), the morphology of the intact and dislocated MRI was quantified.

RESULTS: The inferior glenohumeral ligament experiences changes in surface area following consecutive anterior dislocations. This was supported by the total surface area increasing from the intact state to dislocated state for each specimen. The first specimen increased from 1714 to 1783 mm^2, the second specimen increased from 1158 to 1334 mm^2, and the third specimen increased from 1991 to 2159 mm^2. The divided subregions of the ranged from 85 to 347 mm^2, with the axillary pouches consistently being larger. When averaging the three specimen analyses, the posterior subregions of the capsule experienced the largest surface area change following dislocations. The posterior subregions of the IGHL experienced 15%, 13%, 17%, and 10% changes whereas the anterior subregions experienced only 6%, 0%, 0%, and 13% changes (**Table 1**). Along with numerical analysis, qualitative comparisons could also be made between the 3D geometric models built

from MRI data of the intact and dislocated state. For each specimen, the dislocated model appeared to be larger and have a distorted grid of gadolinium-soaked seeds.

DISCUSSION: The major finding of this study was the tendency for the posterior side of the inferior glenohumeral capsule to experience a larger change in surface area than the anterior side. Quantitatively, the posterior IGHL appeared to experience a more dramatic change in shape than did the anterior side, however, more specimen tests would be required to solidify this finding. This study was consistent with prior literature in that capsular size (volume, surface area) increased following multiple anterior dislocations. Additionally, the 3D MRI models and eight subregions proved to be an applicable technique to use in future studies. For example, a patient with a history of shoulder instability from multiple dislocations is imaged on both shoulders and 3D models are built from the MRI data. The surface area is quantified, and an individualized approach could be taken for their surgical procedure. Ultimately, quantifying the IGHL in several subregions has allowed for a better understanding of the morphology of the entire shoulder joint capsule.

CLINICAL RELEVANCE: By quantifying capsular surface area using the MRI 3D modeling technique, surgical repair on instable shoulders could be individualized directly to the patient's needs. The ability to recognize measurable change and identify the specific subregion of the glenohumeral capsule requiring plication could vastly improve the poor recurrent rate of shoulder injury. Specific knowledge of a patient's IGHL could take objectivity out of surgical repair and specify the targeted region.

REFERENCES: [1] Moore et al. JOR. 2008 [2] Bessiere et al. CORR. 2014 [3] Obrien et al. AJSM. 1995 [4] Yoshida et al. CBM. 2019 [5] Zimmermann et al JBJS. 2016 [6] Hawk et al. ORS. 2019

ACKNOWLEDGMENTS: This research was done at the Orthopedic Robotics Laboratory with assistance from the University of Pittsburgh Department of Bioengineering and Orthopedic Surgery.

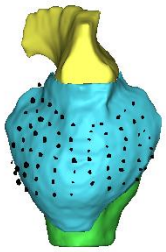

Figure 1: 3D reconstruction of the glenoid (yellow), humerus (green), IGHL (blue), and 77 canola seeds (black).

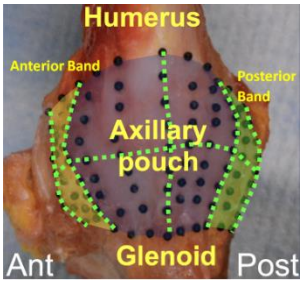

Figure 2: Inferior glenohumeral ligament subregions

ABG	AAPG	PAPG	PBG
6%	0%	15%	13%
0%	13%	17%	10%
ABH	AAPH	PAPH	PBH

Table 1. Average IGHL subregion surface area change from intact to dislocated state. Anterior band of IGHL (AB), anterior axillary pouch (AAP), posterior axillary pouch (PAP), posterior band (PB), glenoid (G), humerus (H).

Quantifying Material Properties of the Patellar Tendon and Quadriceps Tendon in Skeletally Immature Specimens

Jayson J. Baggett[1], Luke T. Mattar[2], Svenja A. Hoger[2], Volker Musahl[2], Richard E. Debski[1,2]

1. Department of Orthopedic Surgery, University of Pittsburgh, Pittsburgh, PA
2. Department of Bioengineering, University of Pittsburgh, Pittsburgh, PA

INTRODUCTION: In recent years there has been a steady increase in ACL injuries amongst the skeletally immature population [1]. ACL reconstruction in pediatrics can be difficult due to risks in damaging the physis and thus the best means of treatment remains a debate [2]. Recent studies show that the use of quadriceps tendon autograft in reconstruction shows promising patient outcomes in regard to postoperative function including a ~90% return to sports rates [3]. In order to restore native knee function, the graft used in reconstruction should imitate the materials properties of the native tissue that the graft is replacing. Although, the material properties of tissue may alter with age and thus choosing the appropriate graft as result may change. Thus, determining the material properties of the quadriceps and patellar tendon in skeletally immature specimens in correlation with age is the purpose of this study.

METHODS: 11 extensor mechanisms (Age: 4.2 ± 3.2 yrs) were dissected from skeletally immature knees. The dissection consisted of removing all soft tissue, fascia, and muscle, leaving just the intact quadriceps tendon, patella, patellar tendon. The extensor mechanisms were then scanned using a 3D laser scanning system (NextEngine 3D scanner HD, Santa Monica, CA) with 2% accuracy and 1.8% repeatability to measure cross-sectional area at the midsubstance of each tendon after being dog-boned to a 7:1 ratio. The extensor mechanisms were then mounted to the material testing machine (Instron Model 5965, Norwood, MA). Beads were placed on the tendon surrounding the midsubstance in addition to both clamps. The beads were tracked during testing using a custom video tracking software (DMAS7, .01 mm accuracy) in order to track the elongation of the tendon. The loading conditions of each specific tendon were determined by applying a specific percentage of the ultimate stress that was found in a previous pediatric tendon study as well as preliminary tests [4]. Both tendons were preloaded (1% of ultimate stress), preconditioned for 20 cycles (1-5% of ultimate stress) and then loaded to failure at 10mm/min. After testing, data processing occurred. Strain was calculated using the 3D position of each bead throughout testing and calculating the distance between the beads surrounding the midsubstance. Cross sectional area of the dog-boned tendon was calculated at the point of failure using MeshLab and used to create stress-strain curves. The tangent modulus, ultimate stress, ultimate strain, and strain energy density were quantified from these plots. The modulus was determined in the linear region of the of the stress-strain curve and the strain energy density was determined using the trapezoid rule from 0% to ultimate strain.

RESULTS: Mechanical testing revealed patellar tendons to exhibit an ultimate stress of 25.4±8.1 MPa, ultimate strain of 12.5%±4.6%, tangent modulus of 309.9±111.4 MPa, and a strain energy density of 1.9± 2.4. Overall, the cross-sectional area at the midsubstance of the central region was 7.8 ± 5.3 mm^2 for the patellar tendons. Quad tendons exhibited an ultimate stress of 18.8±8.3 MPa, a ultimate strain of 11.0%±4.5%, a tangent modulus of 254.5±146.6 MPa, and a strain energy density of 1.1±0.6 MPa. Overall, the cross-sectional area at the midsubstance of the central region was 7.6 ± 4.7 mm^2 for the quad tendons. No correlations between age and material properties were found.

DISCUSSION: The primary findings of the study were that the material properties of the skeletally immature patellar and quadriceps tendons were not associated with age. The lack of change in material properties could be due to the minimal change in microstructure of the tissue or due to the omission of cause of death. Furthermore, the lack of a trend between properties and age could be due to limited sample size. Compared to previous literature [4], the patellar tendon strain calculations found were on average approximately 280% greater than the strain calculations found in this study and the quad tendon strain calculations were on average approximately 350% greater than the strain calculations found in this study. Reasons for variations in these calculations are primarily due to the way strain was calculated in each

study. In other studies strain was calculated using the distance and change in distance between the clamps to calculate strain whereas elongation of the tendon was calculated at the midsubstance for this study in which less elongation was found resulting in a reduction in strain values. Furthermore, this implies that the patellar and quadriceps tendon does not elongate uniformly under tensile loads.

REFERENCES: [1] Weitz et al. KSSTA 2019. [2] McConkey, Musculoskeletal Medicine, 2011, [3] Zakharia A et al. KSSTA 2022, [4] Schmidt EC et al. OJSM 2019.

ACKNOWLEDGEMENT: We gratefully acknowledge the families for their donation of the skeletally immature specimens.

Table 1: Age and material properties of skeletally immature human patellar tendons

Age (years)	Ultimate Stress (MPa)	Ultimate Strain (mm/mm)	Tangent Modulus (MPa)	Strain Energy Density (MPa)
0.1	24.4	0.07	457.8	0.64
0.3	21.7	0.20	161.4	2.80
0.8	17.6	0.20	156.4	1.36
3.1	36.8	0.12	369.6	2.00
3.4	22.6	0.12	282.1	1.70
4	31.6	0.09	377.2	1.33
5.5	13.3	0.07	347.8	0.31
6.2	35.7	0.16	366.9	3.52
7.3	32.1	0.15	285.9	2.44
8	14.8	0.07	378.9	0.59
8.7	29.9	0.13	196.9	1.30

Table 2: Age and material properties of skeletally immature human quadriceps tendon

Age (years)	Ultimate Stress (MPa)	Ultimate Strain (mm/mm)	Tangent Modulus (MPa)	Strain Energy Density (MPA)
0.1	7.2	0.14	63.0	0.90
0.3	9.4	0.04	232.6	0.20
0.8	22	0.17	160.7	1.93
3.1	20.8	0.17	130.1	1.70
3.4	24.2	0.11	256.2	1.30
4	19.5	0.16	155.6	1.80
5.5	13	0.05	368.1	0.40
6.2	30	0.08	461.3	1.00
7.3	12.3	0.07	290.1	0.50
8	28.9	0.08	419.2	0.80
8.7	6.5	0.10	77.8	0.40